Stem Cell Reports
Article

ISSCR

OPEN ACCESS

SIRT1 Enhances the Survival of Human Embryonic Stem Cells by Promoting DNA Repair

Jiho Jang,[1,3] Yong Jun Huh,[1,3] Hyun-Ju Cho,[1,3] Boram Lee,[2] Jaepil Park,[1] Dong-Youn Hwang,[2,*] and Dong-Wook Kim[1,*]

[1]Department of Physiology and Brain Korea 21 Plus Project for Medical Science, Yonsei University College of Medicine, Seoul 03722, Korea
[2]Department of Biomedical Science, CHA University, Seongnam, Kyeonggido 13488, Korea
[3]Co-first author
*Correspondence: hdy@cha.ac.kr (D.-Y.H.), dwkim2@yuhs.ac (D.-W.K.)
http://dx.doi.org/10.1016/j.stemcr.2017.06.001

SUMMARY

Human embryonic stem cells (hESCs) hold great promise for the treatment of many incurable diseases. Sirtuin1 (SIRT1), a class III histone deacetylase, is abundantly expressed in hESCs and is known to regulate early differentiation and telomere elongation. Here, we show that downregulation of SIRT1 promotes cell death in hESCs, but not in differentiated cells, and the SIRT1-inhibition-mediated cell death is preceded by increased DNA damage. This increased DNA damage is at least partially due to decreased levels of DNA repair enzymes such as MSH2, MSH6, and APEX1. Furthermore, SIRT1 inhibition causes p53 activation, which eventually leads to DNA damage-induced apoptosis of hESCs. This study provides valuable insights into the mechanism of SIRT1-mediated hESC survival and should contribute to the development of safe and effective cell therapies.

INTRODUCTION

Human pluripotent stem cells (hPSCs), such as human embryonic stem cells (hESCs) and induced pluripotent stem cells (iPSCs), are characterized by their capacity to proliferate indefinitely and to differentiate into most cell types in the human body. Because of these unique properties, hPSCs hold great promise for the treatment of many incurable diseases through cell replacement therapy (Hwang et al., 2010; Yoo et al., 2013).

Despite more than a decade of intensive research, understanding of the physiology and functional regulation of hPSCs, especially hESCs, remains far from complete. The rapid proliferation of hESCs, which is caused primarily by a shortened G_1 phase and a rapid G_1/S transition, increases the risk of replication errors and enhances the levels of reactive oxygen species within these cells (Becker et al., 2006). A variety of internal factors and external environmental stimuli, such as genotoxic chemicals and physical stimuli (e.g., ionizing radiation, UV light), are potential causes of different forms of DNA damage, such as single-strand breaks, abasic sites, DNA adducts, and double-strand breaks (DSBs) (Houtgraaf et al., 2006). Such DNA damage in turn induces various intracellular responses, such as cell cycle changes, the activation of DNA repair machineries, and apoptosis.

Sirtuin1 (SIRT1) is a nicotinamide adenine dinucleotide (NAD^+)-dependent class III histone deacetylase that is known to regulate stress responses, genomic stability, and cell survival (Chung et al., 2006; Terada et al., 2002; Ying et al., 2002). Previous work has shown that the DNA damage repair system does not function properly in SIRT1 mutant mice (Wang et al., 2008). In addition, several studies have implicated SIRT1 in DNA repair and cell survival in cancer cells (Kalle et al., 2010; Kojima et al., 2008; Lin and Fang, 2013), which is consistent with the abnormal SIRT1 protein levels in many cancer cells (Elangovan et al., 2011; Huffman et al., 2007; Kuzmichev et al., 2005). To date, the role of SIRT1 in hESCs has remained poorly understood. Recent studies have suggested a link between Sirt1 and the differentiation of mouse ESCs (mESCs), hematopoietic stem cells, and mesenchymal stem cells (Calvanese et al., 2010; Lee et al., 2012; Ou et al., 2011; Simic et al., 2013; Tang et al., 2014). In particular, Ou et al. (2011) have reported that Sirt1 knockout mice display defects in hematopoietic differentiation and the formation of a primitive vasculature. Sirt1 has also been shown to enhance the reprogramming of mouse fibroblasts (Lee et al., 2012), facilitate telomere elongation in mouse iPSCs (De Bonis et al., 2014), and maintain the pluripotency of hESCs (De Bonis et al., 2014; Zhang et al., 2014). In addition, SIRT1 has been shown to induce autophagy in response to oxidative stress in both mESCs and hESCs (Ou et al., 2014). To date, most studies regarding the functions of Sirt1 in pluripotent stem cells have been performed using mESCs, and understanding of SIRT1 functions in hESCs remains far from complete. In particular, the roles of SIRT1 in hESC genome stability and survival have yet to be investigated in detail.

In this study, we sought to examine the role of SIRT1 in hESC survival. Using proteomic analysis, we showed that SIRT1 in hESCs critically modulates the levels of two DNA mismatch repair enzymes, MSH2 and MSH3, and a DNA base excision repair enzyme, APEX1, and provided

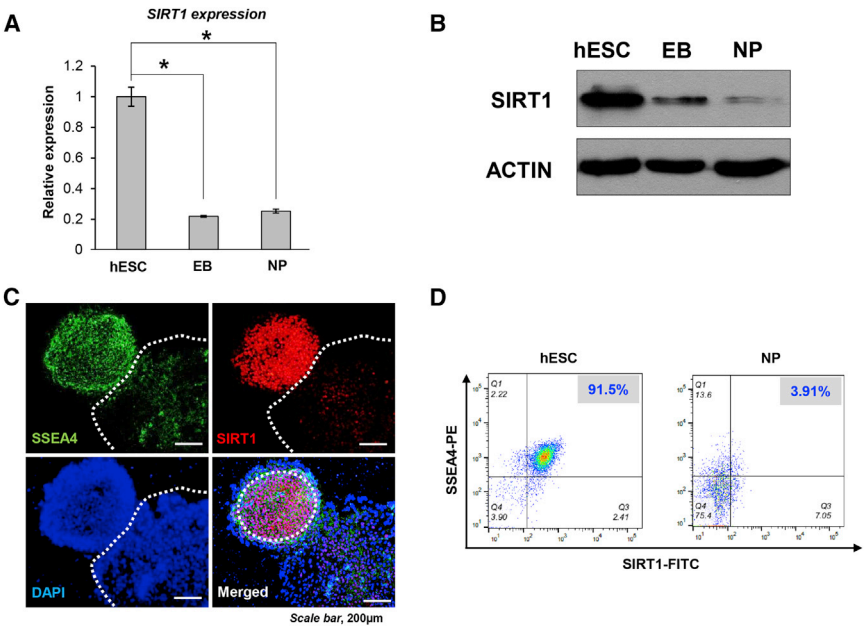

Figure 1. SIRT1 Levels Are High in hESCs and Are Greatly Decreased in Differentiated Cells

(A) *SIRT1* expression levels in hESCs and differentiated cells (EBs and NPs) were measured by qRT-PCR. Decreased *SIRT1* expression was observed in EBs and NPs compared with hESCs. Data are shown as means ± SEM (n = 6 independent experiments; *p < 0.05).

(B) SIRT1 expression levels in hESCs, EBs, and NPs were compared by western blotting.

(C) Immunocytochemistry shows the co-localization of SSEA4 (green) and SIRT1 (red) immunoreactivity sites. The white dashed lines demarcate differentiated cells.

(D) Flow cytometric analysis for SSEA-4 (phycoerythrin, PE) and SIRT1 (fluorescein isothiocyanate, FITC) surface antigen expression was performed on hESCs (left panel) or NPs (right panel). Numbers shown in the individual quadrants indicate the percentage of cells of each type.

evidence that SIRT1 is critically implicated in DNA repair processes that in turn affect the genome stability and survival of hESCs.

RESULTS

SIRT1 Is Abundantly Expressed in hESCs

Previous reports have shown that Sirt1 protein regulates the pluripotency and differentiation of mESCs (Ou et al., 2011; Zhang et al., 2014). We first compared the level of SIRT1 among hESCs and their differentiated derivatives, such as embryoid bodies (EBs) and neural precursors (NPs). qRT-PCR showed that *SIRT1* mRNA levels were at least 4-fold higher in hESCs than in EBs and NPs (Figure 1A). Western blotting also showed that SIRT1 protein levels were significantly higher in hESCs than in EBs and NPs (Figure 1B). Furthermore, immunocytochemistry clearly showed that SIRT1 was strongly expressed in undifferentiated ($SSEA4^+$) hESCs (Figure 1C, top two panels), whereas its expression was drastically decreased in a large population of differentiated ($SSEA4^-$) cells (Figure 1C, top panels, the areas surrounded by white dotted lines). A merged image clearly showed that most sites of SIRT1 and SSEA4 immunoreactivity were co-localized (Figure 1C, bottom right panel, inside the white dotted circle).

Flow-cytometric analysis showed that most hESCs (~91.5%) displayed immunoreactivity toward both SSEA4 and SIRT1, thus demonstrating co-expression of SSEA4 and SIRT1in hESCs at a cellular level (Figure 1D, left panel). However, the expression of both markers was simultaneously downregulated (i.e., $SSEA4^+$ $SIRT1^+$ = ~3.91%, $SSEA4^-$ $SIRT1^-$ = ~75.4%) in NPs that were differentiated from hESCs (Figure 1D, right panel).

Together, our results demonstrated a high SIRT1 level in hESCs but not in differentiated cells (i.e., EB and NPs). This dramatic change in SIRT1 level suggested that Sirt1 is critically involved in the physiology of hESCs.

SIRT1 Inhibition Induced Apoptosis in hESCs

SIRT1 has been reported to decrease apoptotic cell death in cancer cells (Kalle et al., 2010; Kojima et al., 2008). In this study, we hypothesized that one of the functions of SIRT1 in hESCs might be to protect the cells from apoptotic cell death. To elucidate the potential involvement of SIRT1 in hESC survival, we examined how knocking down the level or inhibiting the function of SIRT1 affected hESC survival/death. First, western blotting confirmed that hDFs, which were used as a negative control (i.e., differentiated cells), did not express SIRT1, whereas hESCs displayed significant SIRT1 expression (Figure 2A).

When hESCs were treated for 12 hr with Tenovin-6, a SIRT1/2 inhibitor, hESCs in compact colonies were severely damaged (Figure 2B, top right panel), whereas hDFs remained intact under the same conditions (Figure 2B, bottom right panel). Next, we observed that a 12-hr treatment with Tenovin-6 induced a significant increase in cleaved caspase-3 (C-CAS3), an apoptotic marker, in hESCs, but not in hDFs (Figure 2C). Flow-cytometric analysis using annexin V and propidium iodide (PI) to evaluate apoptosis showed a significant increase in apoptotic cells after Tenovin-6 (5 μM, 12 hr) treatment in hESCs (i.e., from

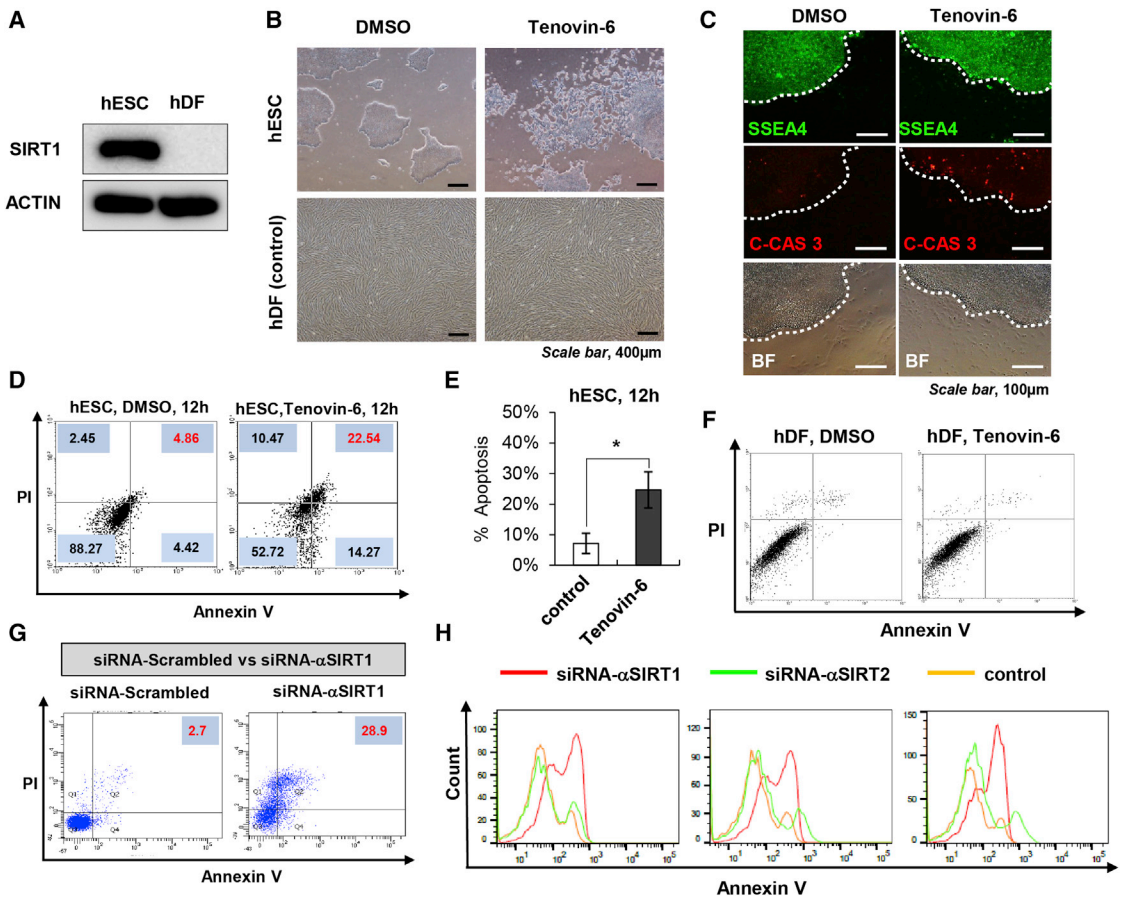

Figure 2. Tenovin-6 Treatment Leads to Cell Death in hESCs but Not in Differentiated Cells

(A) A representative immunoblot showing the difference in SIRT1 expression level between undifferentiated cells (hESCs) and fully differentiated cells (hDFs).

(B) Typical phase-contrast images of hESCs and hDFs were taken after Tenovin-6 (5 μM) treatment for 12 hr.

(C) Immunocytochemistry showed that cleaved caspase-3 (C-CAS 3) immunoreactivity dramatically increased after Tenovin-6 treatment (2 μM, 12 hr). The areas surrounded by white dashed lines demarcate the areas composed of undifferentiated hESCs.

(D) Flow cytometric analysis of hESCs was performed after Tenovin-6 treatment (5 μM, 12 hr). y Axis, propidium iodide (PI); x axis, annexin V (FITC-labeled).

(E) Percentages of apoptotic cells obtained from flow-cytometric analysis of hESCs treated with Tenovin-6 (5 μM, 12 hr). Data are shown as means ± SEM (n = 6 independent experiments; *$p < 0.05$).

(F) Flow-cytometric analysis of hDFs was performed after Tenovin-6 treatment (5 μM, 12 hr). y Axis, PI; x axis, annexin V (FITC-labeled).

(G) Flow-cytometric analysis of apoptotic cells using PI and an annexin V antibody was performed at 48 hr after transfection with siRNA-αSIRT1.

(H) The three histograms derived from each independent flow cytometric analysis are shown. In the experiments, the number of apoptotic cells was counted at 48 hr after transfection of hESCs with either siRNA-αSIRT1 or siRNA-αSIRT2. An FITC-conjugated annexin V antibody was used for the analysis (n = 3 independent experiments).

~4.86% to ~22.54%) (Figures 2D and 2E), but not in hDFs (Figure 2F). Repeated experiments consistently showed that the percentage of apoptotic cells was significantly increased after Tenovin-6 treatment in a time-dependent manner, reaching nearly 40% at 16 hr post treatment (Figures S1A and S1B). Moreover, treatment of hESCs and hDFs with other SIRT1 inhibitors, such as Sirtinol (50 μM), Salermide (50 μM), and EX527 (5 μM), also induced cell death of only hESCs without affecting hDFs (Figure S1C). Because EX527 is a selective SIRT1 inhibitor that does not block other SIRT family proteins, it is evident that SIRT1 inhibition induces hESC death (Figure S1C, top rightmost panel).

To further confirm the involvement of SIRT1 in the regulation of hESC death, we specifically knocked down *SIRT1*

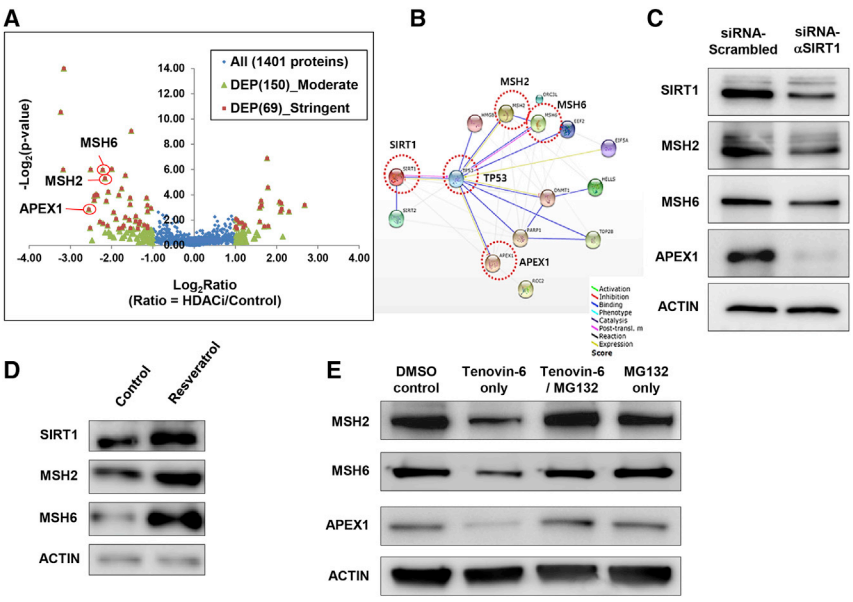

Figure 3. Proteomic Analysis Showed that SIRT1 Inhibition Significantly Decreased DNA Repair Proteins in hESCs

(A) Volcano plot of differentially expressed proteins (DEPs) between control and SIRT1-inhibited groups. Fold change (in $\log_2$) is plotted against the Edge R-generated p value (log base 2). Differential expression analysis identified 219 DEPs between the control and SIRT1-inhibited groups: a total of 140 and 79 proteins were downregulated and upregulated by SIRT1 inhibition, respectively. The 140 downregulated proteins were divided into 46 stringently regulated proteins (red-brown squares, $\log_2 < -1$, $p < 1.0 \times 10^{-0.2}$) and 94 moderately regulated proteins (pear-green triangles, $-1 < \log_2 < 0$, $p < 1.0 \times 10^{-0.2}$). Likewise, the 79 upregulated proteins were divided into 23 stringently regulated proteins (red-brown squares, $\log_2 > 1$, $p < 1.0 \times 10^{-0.2}$) and 56 moderately regulated proteins (pear-green triangles, $0 < \log_2 < 1$, $p < 1.0 \times 10^{-0.2}$).

(B) The protein-protein interaction biochemical network was generated using the STRING database (Search Tool for the Retrieval of Interacting proteins) (http://string-db.org/) and provided information on proteins that either directly or indirectly interact with SIRT1.

(C) Western blotting of SIRT1, MSH2, MSH6, and APEX1 was performed at 12 hr post transfection.

(D) Representative western blotting of hESCs treated with resveratrol (10 μM) for 24 hr was performed to examine the levels of SIRT1 and DNA repair proteins (MSH2 and MSH6).

(E) Western blotting of MSH2, MSH6, and APEX1 was performed after hESCs were treated with a combination of a SIRT1 inhibitor and/or a proteasome inhibitor (DMSO only, Tenovin-6 only, Tenovin-6 + MG132, and MG132 only).

using an *SIRT1*-specific small interfering RNA (siRNA-αSIRT1) and examined the degree of cell death by flow-cytometric analysis using an annexin V antibody and PI (Figure 2G). The knockdown specificity of siRNA-αSIRT1 used in this experiment was confirmed because it decreased only the *SIRT1* mRNA level (Figure S2A). After transfection of hESCs with siRNA-αSIRT1, the *SIRT1* mRNA level was decreased in a reverse time-dependent manner, probably because of the degradation of transfected siRNA-αSirt1 over time (Figure S2B). At 48 hr after siRNA-αSIRT1 transfection, we still observed a significant number of apoptotic cells (2.7%, siRNA-Scrambled versus 28.9%, siRNA-αSIRT1) (Figure 2G).

When we examined the contribution of SIRT2 to hESC survival/death by using an siRNA specific for *SIRT2* (Figure S2C), no significant induction of cell death was detected (Figure 2H), thus suggesting that SIRT2 plays only a marginal role in the regulation of hESC survival. This result also indicated that a large portion of cell death induced by Tenovin-6 treatment (i.e., inhibition of SIRT1 and 2) is caused by blocking SIRT1 (Figure 2H).

Together, our results demonstrated that either blocking the function or decreasing the level of SIRT1 robustly enhanced hESC death, thus indicating that SIRT1 is critical for the survival of hESCs.

Proteomic Analysis Showed that SIRT1 Inhibition Significantly Decreased DNA Repair Proteins in hESCs

To gain mechanistic insight into the early events occurring after SIRT1 inhibition, we treated hESCs with Tenovin-6 for 2 hr and performed proteomic analysis. A total of 1,401 different proteins were identified using isobaric tags for relative and absolute quantification (iTRAQ)-based proteomic analysis. Of these, 140 and 79 proteins were downregulated and upregulated, respectively, in hESCs treated with Tenovin-6 compared with cells treated with DMSO (control) (Figure 3A and Tables S1–S4). The 140 downregulated proteins were divided into 46 stringently regulated proteins (red-brown squares) and 94 moderately regulated proteins (pear-green triangles) (Figure 3A, left half; Tables S1 and S2). Likewise, the 79 upregulated proteins were divided into 23 stringently regulated proteins (red-brown squares) and 56 moderately regulated proteins (pear-green triangles) (Figure 3A, right half; Tables S3 and S4).

Next, we performed KEGG pathway enrichment analysis and found that the enriched categories included pathways involved in DNA repair. Notably, MSH2 and MSH6, which are involved in repairing DNA base mismatches, and APEX1, which has been implicated in DNA excision repair, were found in the stringently downregulated group (Figure 3A). The protein-protein interaction biochemical

network generated using the STRING database (Search Tool for the Retrieval of Interacting proteins database) (http://string-db.org/) provided information on proteins that either directly or indirectly interact with SIRT1. Analysis of this protein network showed that SIRT1 was closely linked to several important DNA repair proteins, including MSH2, MSH6, and APEX1 (Figure 3B).

Together, these results suggest the intriguing possibility that SIRT1 interacts with several DNA repair proteins and that these interactions may be responsible for SIRT1-mediated hESC survival.

Proteomic Analysis Data Were Validated by Western Blotting

We first examined whether our proteomic data were reliable. To this end, we chose several up- and downregulated proteins and validated the expression of these proteins by using western blotting. All four upregulated proteins examined, PDI, T-PLASTIN, VDAC1, and VIMENTIN, were detected at a higher level in Tenovin-6-treated hESCs than in control (DMSO-treated) hESCs (Figure S3A). In addition, the levels of four downregulated proteins, MTHF1, MYOSIN, FILAMIN1, and EZRIN, were lower in Tenovin-6-treated hESCs than in control hESCs (Figure S3B). These western blot results confirmed the validity of our proteomic data.

Next, we examined the levels of the three DNA repair proteins, MSH2, MSH6, and APEX1, which were shown to be downregulated by Tenovin-6 treatment in our proteomic analysis. For western blotting, we transfected hESCs with siRNA-Scrambled and siRNA-αSIRT1 and collected samples at 12 hr post transfection. As expected, the protein levels of SIRT1, MSH2, MSH6, and APEX1 were decreased in cells transfected with siRNA-αSIRT1 (Figure 3C).

To further confirm the role of SIRT1 in regulating the protein expression of MSH2, MSH6, and APEX1, we elevated the SIRT1 protein level by treating hESCs with resveratrol, a SIRT1 activator. Our western blotting results showed that increasing SIRT1 by resveratrol treatment upregulated DNA repair proteins such as MSH2 and MSH6 (Figure 3D).

Intriguingly, the *MSH2*, *MSH6*, and *APEX1* mRNA levels did not decrease after Sirt1 knockdown (data not shown). This observation contrasted with the decreased protein levels of these DNA repair genes after SIRT1 inhibition, thus suggesting the involvement of post-transcriptional regulation.

To understand the mechanisms underlying the decrease in DNA repair proteins without the decrease in their respective mRNAs after SIRT1 inhibition, we tested whether SIRT1 inhibition induced the proteasomal degradation of these DNA repair enzymes. To this end, we treated cells with Tenovin-6 along with a proteasome inhibitor, MG132. The significant decrease in DNA repair proteins after Tenovin-6 treatment did not occur when MG132 was also added, thus indicating that proteasomal degradation is involved in the SIRT1-mediated regulation of DNA repair enzyme levels (Figure 3E). This result suggested that the decrease in the three DNA repair proteins, MSH2, MSH6, and APEX1, after SIRT1 inhibition was at least partly due to enhanced proteasomal degradation.

Together, our data demonstrated that a high level of SIRT1 protein in hESCs increases several DNA repair proteins and the proteasomal degradation pathway is at least partly involved in the SIRT1-mediated regulation of the DNA repair proteins.

SIRT1 Inhibition Increased DNA Damage in hESCs

Because we found a link between the levels of SIRT1 and DNA repair proteins, we examined whether blocking SIRT1 activity eventually leads to increased DNA damage. First, we performed apurinic/apyrimidinic (AP)-site staining of hESCs after Tenovin-6 treatment (5 μM, 12 hr): AP sites are the most common form of single-strand DNA damage (Demple and Harrison, 1994). Tenovin-6-treated hESCs displayed a large number of AP-site-positive cells, whereas control (DMSO-treated) cells showed no prominent AP sites (Figure 4A, upper two panels and graph). As a positive control, hESCs were treated with epigallocatechin gallate (EGCG), which reacts with the culture medium and generates hydrogen peroxide (H_2O_2) and further causes DNA damage (Figure 4A, lower two panels). These results suggested that SIRT1 inhibition causes a concomitant increase in single-strand DNA breaks in hESCs.

Next, we sought to examine whether SIRT1 inhibition in hESCs might promote more severe DNA damage such as DNA DSBs, which are known to cause apoptotic cell death (Roos and Kaina, 2006). Phosphorylated H2AX (γ-H2AX) is a good indicator of DSBs, because DSBs are typically followed by histone H2AX phosphorylation (Kinner et al., 2008). Treatment of hESCs with Tenovin-6 for 12 hr increased the number of γ-H2AX$^+$ cells in a dose-dependent manner (Figures 4B and 4C). Nuclear staining with DAPI showed that the compact colony morphology was lost at high concentrations of Tenovin-6 (i.e., 5 μM and 10 μM) (Figure 4B, lower panels). By contrast, hDFs did not display any morphological changes at the high concentrations of Tenovin-6 used in this study (i.e., 5 μM) (Figure S4A), in agreement with the results in Figures 2B and 2F. In addition, few γ-H2AX$^+$ cells were detected in hDFs after Tenovin-6 (5 μM) treatment (Figure S4A).

To examine the correlation between DNA damage and cell death, we examined the number of γ-H2AX$^+$ and Dead Green$^+$ (a marker for cell death) cells at both 2 hr and 6 hr. At 2 hr post treatment, some γ-H2AX$^+$ cells were observed, whereas few Dead Green$^+$ cells appeared (Figures S4B [upper panels] and 4D). A significant number

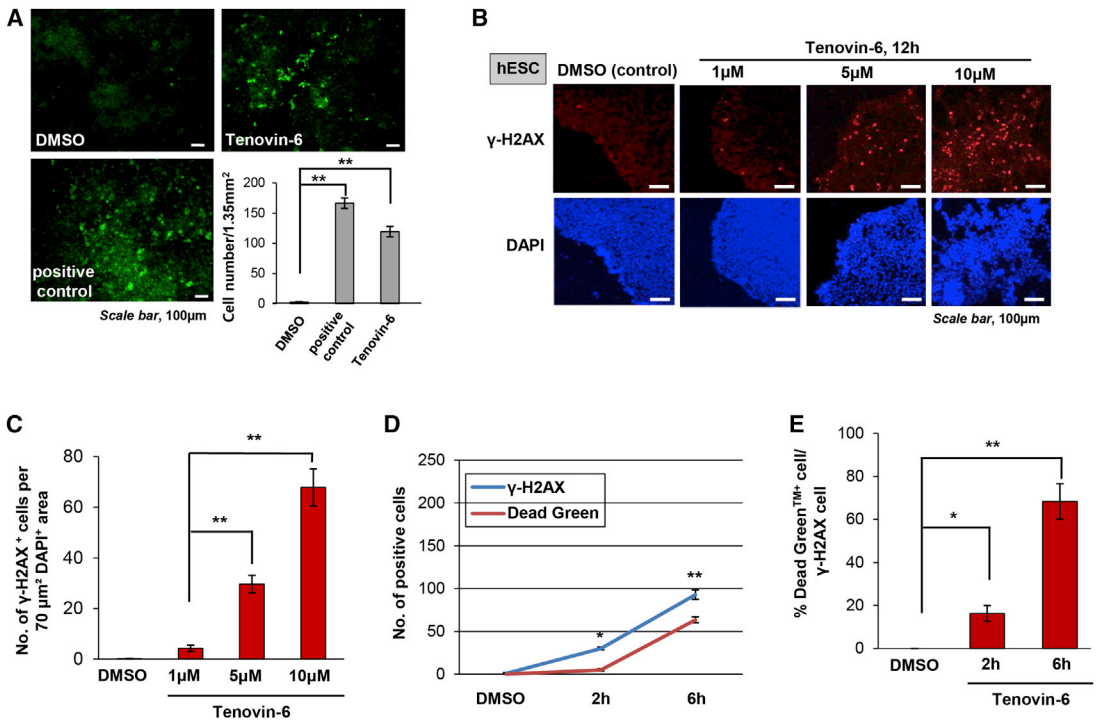

Figure 4. Tenovin-6 Treatment Induces DNA Damage in hESCs

(A) Immunofluorescence analysis of AP (apurinic/apyrimidinic) sites in hESCs treated with Tenovin-6 (5 μM, 12 hr) and EGCG (5 μM, 12 hr) as a positive control. The data were quantified and are presented in a graph (lower right panel). Data are shown as means ± SEM (n = 3 independent experiments; **p < 0.01).

(B) Immunofluorescence analysis showed that the number of hESCs containing DSBs (γ-H2AX$^+$) also increased in a dose-dependent manner after Tenovin-6 treatment.

(C) The number of γ-H2AX$^+$ cells per 70 μm^2 DAPI$^+$ area is presented as a bar graph. Data represent means ± SEM (n = 3 independent experiments; **p < 0.01).

(D) The numbers of Dead Green$^+$ and γ-H2AX$^+$ cells were counted at 2 hr and 6 hr after Tenovin-6 (5 μM) treatment and plotted in the graph. Data represent means ± SEM (n = 6 independent experiments; *p < 0.05, **p < 0.005).

(E) The percentages of the total γ-H2AX$^+$ cells that were Dead Green$^+$ were measured and presented as a bar graph. Data are shown as means ± SEM (n = 6 independent experiments; *p < 0.01, **p < 0.001).

of Dead Green$^+$ cells and γ-H2AX$^+$ cells were detected at 6 hr, and γ-H2AX$^+$ cells outnumbered Dead Green$^+$ cells (Figures S4B [lower panels] and 4D). Intriguingly, a large portion of γ-H2AX$^+$ cells were positive for Dead Green at 6 hr (>60%) (Figure 4E), and no Dead Green$^+$ γ-H2AX$^-$ cells were detected (Figure S4B), thus indicating the close relationship between DSB DNA damage and cell death after Tenovin-6 treatment. In addition, H2AX phosphorylation preceded cell death in hESCs (Figures 4D and S4B), thus further suggesting that DNA DSBs were at least partly responsible for cell death after SIRT1 inhibition. These results confirmed that Tenovin-6 treatment resulted in increased DNA damage (i.e., DSBs) and subsequent apoptotic cell death.

Because Tenovin-6 inhibits the functions of both SIRT1 and SIRT2 (Lain et al., 2008), we examined the effect of only SIRT1 by specifically knocking down *SIRT1* mRNA by using siRNA-αSIRT1. As expected, DNA DSBs were drastically increased at 24 and 48 hr after siRNA-αSIRT1 transfection in hESCs, but not in hDFs (Figures 5A and 5B).

In addition, enhancement of SIRT1 expression by resveratrol treatment decreased the oxidative stress (H_2O_2)-induced increase in DNA DSBs, thus indicating a clear role of SIRT1 in the decrease in DNA damage (Figure 5C).

Together, our results demonstrated that SIRT1 plays a critical role in preventing DNA damage in hESCs, which in turn protects hESCs from death.

SIRT1 Knockdown Marginally Induced hESC Differentiation

To determine whether SIRT1 is involved in hESC differentiation, as previously shown (De Bonis et al., 2014; Zhang et al., 2014), we analyzed hESCs at 72 hr after

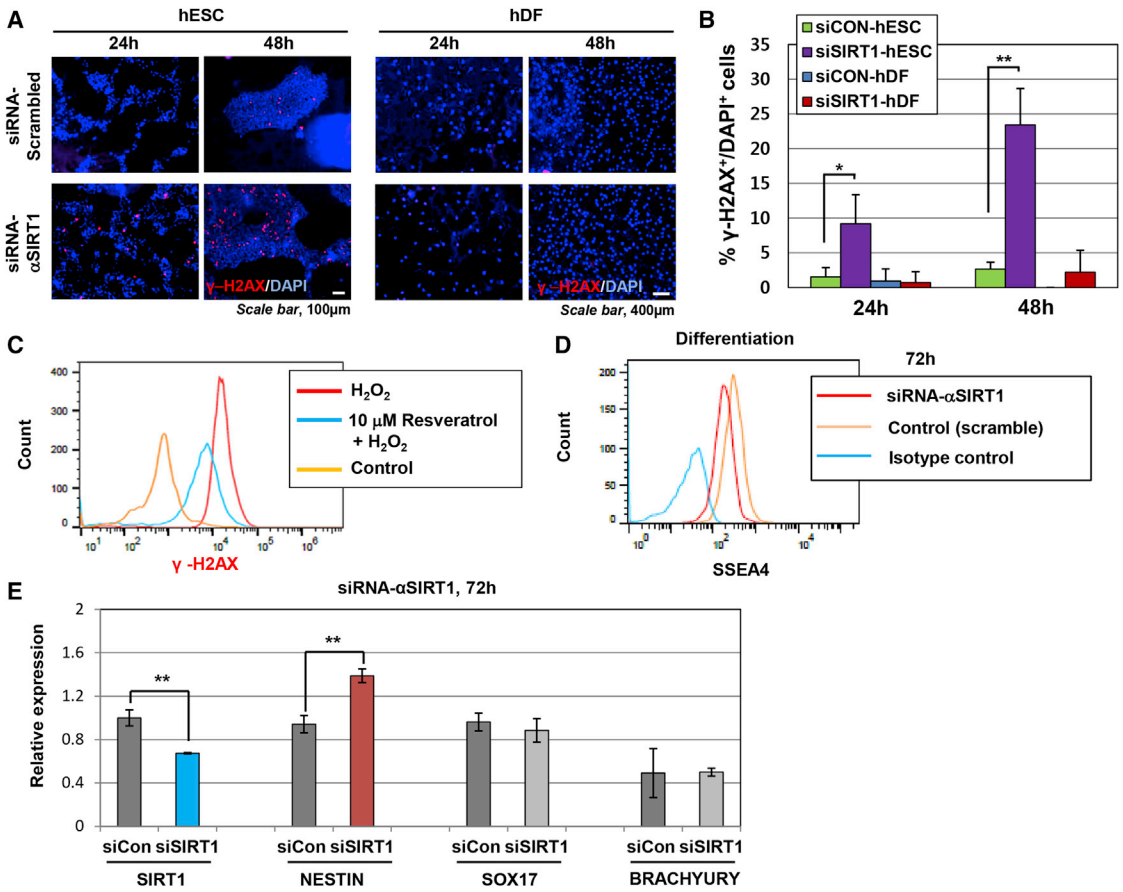

Figure 5. SIRT1 Plays a Major Role in Genome Stability and Is Marginally Involved in hESC Differentiation

(A) Immunofluorescence images showing the numbers of hESCs and hDFs with DSB DNA damage (γ-H2AX$^+$) at 24 hr and 48 hr after transfection with siRNAs (siRNA-Scrambled and siRNA-αSIRT1).

(B) Percentages of total cells (DAPI$^+$ cells) that were γ-H2AX$^+$. Data are shown as means ± SEM (n = 6 independent experiments; *p < 0.01, **p < 0.001).

(C) Histogram showing intracellular γ-H2AX$^+$ levels of hESCs treated with 2.5 mM H_2O_2 in the absence or presence of resveratrol pre-treatment (10 μM, 24 hr).

(D) The level of SSEA-4 (phycoerythrin, PE), an undifferentiated cell marker, was examined using flow-cytometric analysis at 72 hr after transfection with siRNAs (siRNA-Scrambled and siRNA-αSIRT1).

(E) Real-time qPCR analysis of the mRNA levels of *SIRT1*, *NESTIN*, *SOX17*, and *BRACHYURY* genes at 72 hr after transfection with siRNAs (siRNA-Scrambled [siCon] and siRNA-αSIRT1). Data are shown as means ± SEM (n = 3 independent experiments; **p < 0.005).

transfection with siRNA-αSIRT1. Our flow cytometric analysis displayed a slight decrease in the SSEA4$^+$ (undifferentiated) cell population after *SIRT1* knockdown (Figure 5D), thus indicating a slight induction of differentiation by *SIRT1* knockdown. Furthermore, we detected an increase in *NESTIN*, a neuroectoderm marker, whereas mesoderm and endoderm lineage markers were not changed (Figure 5E).

Our results together showed some evidence of hESC neural differentiation, although the most dramatic effects detected after SIRT1 inhibition or knockdown were increased DNA damage and subsequent cell death.

Tenovin-6-Mediated p53 Acetylation Was Not Required for the Early Decrease in DNA Repair Proteins

We already showed that SIRT1 inhibition induced apoptotic cell death of hESCs (Figure 2). Because DNA damage activates p53 through acetylation (Sakaguchi et al., 1998), which in turn results in apoptosis (Sykes et al., 2006; Tang et al., 2006), we examined whether Tenovin-6 treatment might promote p53 acetylation with subsequent induction of apoptosis in hESCs. Our western blotting analysis showed that the levels of acetylated (activated) p53 and cleaved caspase-3 were significantly increased after Tenovin-6 treatment (5 μM, 12 hr) in hESCs, but not in

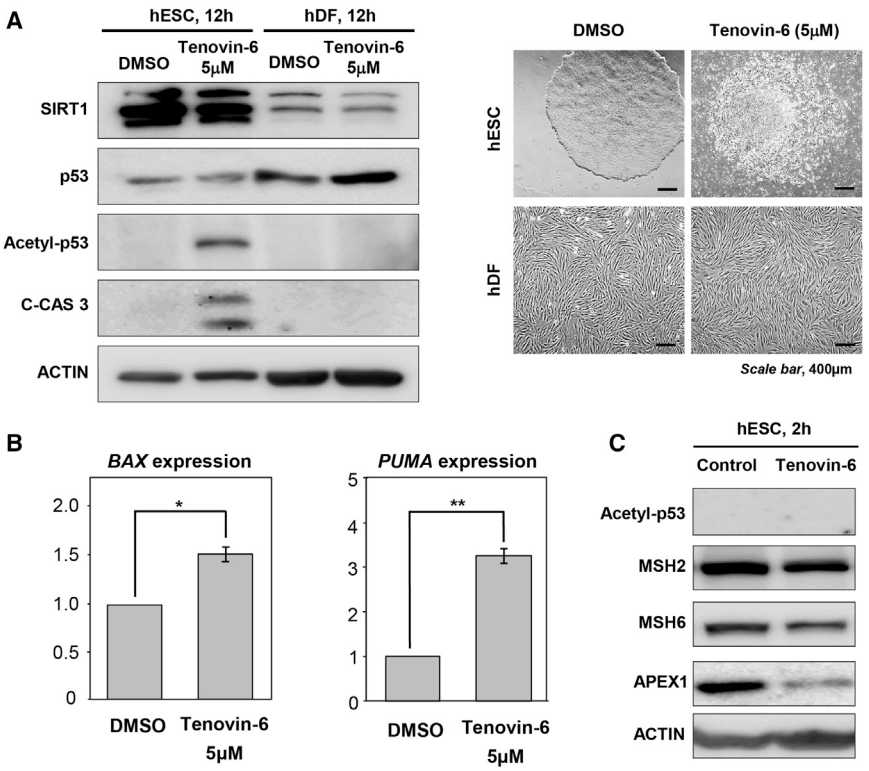

Figure 6. Tenovin-6-Mediated p53 Acetylation Was Not Required for the Early Decrease in DNA Repair Proteins

(A) Western blotting for p53 (a known target of SIRT1), acetylated-p53 (an active form of p53), and cleaved caspase-3 (an apoptotic marker) was performed in cells with or without Tenovin-6 treatment (5 μM, 12 hr) (left panel). The morphologies of the cells used for western blotting are shown on the right.

(B) Expression levels of *PUMA* and *BAX*, two pro-apoptotic genes, were examined by real-time qPCR in cells with or without Tenovin-6 treatment (5 μM, 12 hr). Data represent means ± SEM (n = 3 independent experiments; *p < 0.05, **p < 0.005).

(C) Western blotting for SIRT1, acetylated p53 (acetyl-p53), MSH2, MSH6, APEX1, and actin (a loading control) was performed at 2 hr after treatment with Tenovin-6 (5 μM).

hDFs (Figure 6A). This result was consistent with our previous immunostaining and flow cytometry data showing a significant increase in hESC death at 12 hr after Tenovin-6 treatment (Figure 2). Our qRT-PCR results showed that SIRT1 inhibition increased the expression of *PUMA* and *BAX*, pro-apoptotic p53 target genes, in hESCs (Figure 6B), thus indicating a connection between SIRT1 inhibition and p53-mediated apoptosis of hESCs.

We next examined whether the decrease in the DNA repair proteins after Tenovin-6 treatment occurred through p53 acetylation. To detect which event occurs first, we performed western blotting at an early time point after Tenovin-6 treatment. In this experiment we examined only an acetylated form of p53, because Lain et al. (2008) have shown that Tenovin-6 does not change the level of total p53 (as seen also in our data, Figure 6A) and does not activate p53 by phosphorylation. Strikingly, treatment of hESCs with Tenovin-6 for 2 hr resulted in a decrease in MSH2, MSH6, and APEX1 proteins, whereas no acetylated form of p53 was apparent at this time point (Figure 6C). This result suggested that the decrease in the DNA repair proteins does not require p53 activation, at least during the early stage.

Together, our results indicated no evidence of a functional connection between acetylated p53 and the decrease in DNA repair proteins. It is plausible that the DNA damage-induced apoptosis after SIRT1 inhibition in hESCs occurs through a p53-independent mechanism, at least during early events (i.e., decrease in DNA repair proteins). This study provides valuable insights into the mechanism underlying the SIRT1-mediated survival of hESCs.

DISCUSSION

hESCs have unlimited proliferation potential and typically have a shorter cell cycle (approximately 15.8 hr) than most somatic cells (24–32 hr), owing to a shortened G_1 phase (approximately 2.5–3 hr) and a faster G_1/S transition (Becker et al., 2006). hESCs retain pluripotency because they are derived from the inner cell mass of blastocysts, which can generate any type of cell in the human body after full development.

It may be reasonable to speculate that cells from early developmental stages (i.e., cells that constitute the inner cell mass and hESCs) retain efficient DNA repair systems, because the introduction of DNA defects during early developmental stages would be disastrous and lead to inherited mutations in differentiated cells. In support of this idea, mESCs have been reported to show more efficient DNA repair activity than fibroblasts after oxidative stress- and ionizing radiation-induced DNA damage (Saretzki et al., 2004). Furthermore, hESCs are prone to undergo apoptosis at lower doses of IR exposure than

somatic cells, thus decreasing the chances of propagating abnormal cells with DNA defects. These observations suggest that hESCs have a fail-safe strategy to decrease cells with defective genetic information by boosting DNA repair systems and/or inducing apoptosis of defective cells (Filion et al., 2009; Sokolov et al., 2012; Wilson et al., 2010). These fail-safe strategies are of great importance in allowing hESCs to avoid any disastrous outcomes derived from the propagation of cells into different cell types with DNA abnormalities. Cells constantly undergo DNA damage in the form of nucleotide changes, abasic sites, and single-strand breaks. If these defects are not efficiently corrected, they eventually form lethal DSBs during DNA replication, when replicative DNA polymerases encounter single-strand breaks. DSBs are extremely detrimental to cells and often cause chromosomal translocations, which are associated with tumor formation and even cell death (Kaina, 2003; Khanna and Jackson, 2001; Rich et al., 2000; Richardson and Jasin, 2000). In response to DNA damage, hESCs arrest at the G_2/M checkpoint, activate DNA repair systems such as BER, MMR, and DSB repair, and finally induce apoptosis, depending on the severity of damage or the success of the DNA repair processes (Liu et al., 2014; Momcilovic et al., 2010).

In our study we found that SIRT1 was required for hESC survival, because SIRT1 inhibition robustly induced apoptotic cell death. Strikingly, we found that inhibiting SIRT1 activity dramatically decreased the level of three DNA repair proteins, MSH2, MSH6, and APEX1. Both MSH2 and MSH6 are principal components of MutS (e.g., the mismatch repair complex), and MutS dysfunction leads to single-strand DNA damage (Westmoreland and Resnick, 2013). APEX1 is a major component of BER, and APEX1 malfunction also leads to single-strand DNA damage (Hable et al., 2012). The single-strand DNA damage generated by SIRT1 inhibition became DSBs and eventually caused apoptosis. In accordance with this finding, resveratrol treatment increased the expression of SIRT1 and, hence, DNA repair proteins (Figure 3D), thereby decreasing DSBs in response to genotoxic stress (Figure 5C). Evidently, this observation was in agreement with findings from a previous report indicating that SIRT1 overexpression leads to increased survival after oxidative stress (Oberdoerffer et al., 2008). Consequently, our findings indicated that SIRT1 is a critical regulator in the orchestration of multiple DNA repair systems and is important for maintaining genomic fidelity and integrity in hESCs.

One important issue to consider is whether p53 plays a critical role in the associations among SIRT1 inhibition, DNA damage induction, and DNA damage-mediated apoptosis. On the basis of previous reports showing that SIRT1 inhibition activates p53 through acetylation, it is conceivable that Tenovin-6 treatment enhances p53 acetylation in hESCs, which in turn leads to (1) a rapid decrease in DNA damage repair proteins, (2) a subsequent increase in DNA damage, and (3) DNA DSB-mediated apoptosis. To resolve this issue, we examined the levels of acetylated p53 and the three DNA repair proteins in hESCs at an early time point (i.e., 2 hr) after Tenovin-6 treatment. Strikingly, the levels of all three DNA repair proteins analyzed, MSH2, MSH6, and APEX1, were rapidly decreased in the absence of p53 acetylation, thus suggesting that acetylated p53 may not be responsible for the rapid decrease in the DNA repair proteins (Figure 6C). Intriguingly, we observed DSBs as early as 2 hr after Tenovin-6 treatment (Figure S4B), thus also indicating that DNA DSBs begin forming rapidly in the absence of acetylated p53. Therefore, it is plausible that activation of p53 by SIRT1 inhibition may not be involved in early events (i.e., decrease in DNA repair proteins and induction of DNA damage) but may be involved in the late stage (i.e., DSB-mediated apoptosis) of SIRT1/DNA damage-mediated apoptosis (Figure 7).

At this stage, we do not fully understand how SIRT1 modulates the level of DNA repair proteins. However, our results demonstrated a connection between SIRT1 and the proteasome pathway. Although beyond the scope of this study, it would be interesting to unveil the detailed mechanism explaining the link between SIRT1 and the proteasome-mediated decrease in DNA repair proteins.

In summary, our study showed that SIRT1 is indispensable for hESC survival and that the modulation of the levels of multiple DNA repair proteins is at least partially responsible for the SIRT1-mediated prevention of cell death (Figure 7). Given the ever-increasing importance of hESCs as a cell source for replacement therapy, this study offers valuable insight into the growth and maintenance of DNA damage-free hESCs for clinical applications.

EXPERIMENTAL PROCEDURES

Culture of hESCs

The human ESC line H9 (WiCell) was cultured in hESC medium containing DMEM-F12 supplemented with 20% Knockout-Serum Replacement medium (Invitrogen), 1× non-essential amino acids (Invitrogen), 0.1 mM β-mercaptoethanol (Sigma), and 4 ng/mL basic fibroblast growth factor (bFGF) (Invitrogen) on a layer of mitotically arrested STO cells (ATCC). hESC colonies were transferred onto fresh feeder cells every 7 days by either a mechanical method or enzymatic passaging using collagenase type IV (Sigma). For feeder-free culture, hESCs were cultured on Matrigel-coated dishes in TeSR-E8 medium (STEMCELL Technologies). All the hESC experiments were approved by the Institutional Ethical Committee, Yonsei University College of Medicine (4-2015-1097).

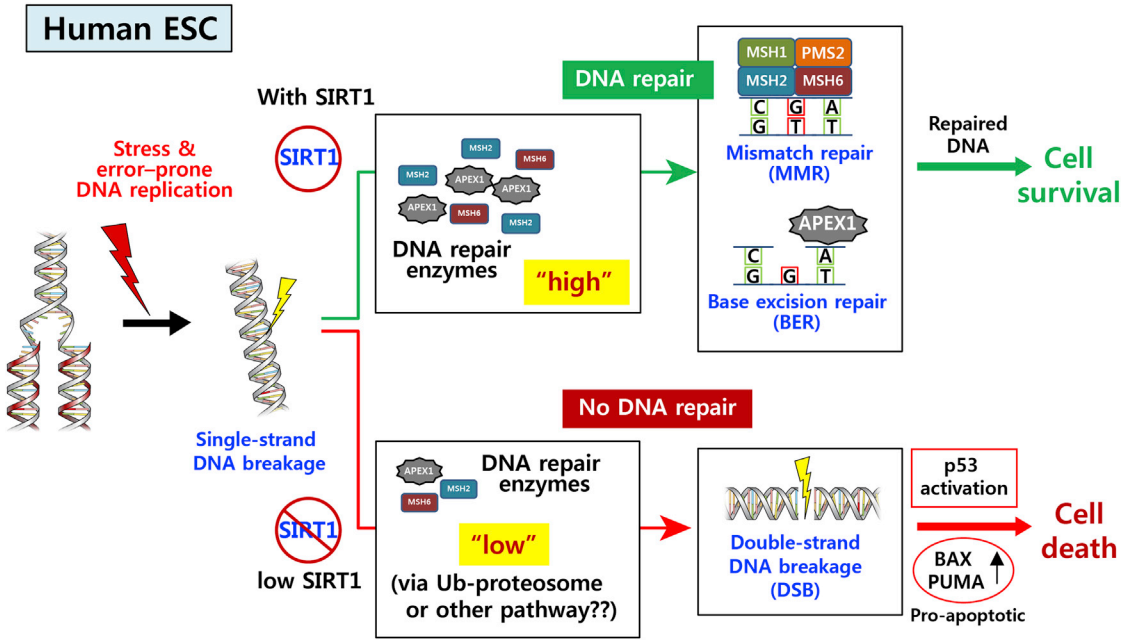

Figure 7. The Mechanism Underlying the Role of SIRT1 in hESC Survival

A high activity/level of SIRT1 in hESCs maintains sufficient levels of certain DNA repair enzymes. For example, we detected a significant decrease in MSH2 and MSH6 as well as APEX1 after inhibition or knockdown of SIRT1. The efficient repair of genetic aberrations by these DNA repair proteins prevents small mutations from progressing into hazardous DSBs, which eventually lead to cellular apoptosis. In the absence of SIRT1 activity in hESCs, the level of several DNA repair enzymes is rapidly decreased by the proteasome and/or another unknown pathway. The early rapid decrease in the DNA repair proteins does not appear to be mediated by acetylated p53. The lack of sufficient DNA repair allows DSB DNA damage to dramatically increase, and this is followed by increased cell death. Acetylation of p53 and concomitant *BAX* and *PUMA* overexpression have been implicated in the DNA damage-mediated apoptosis.

Differentiation of hESCs *In Vitro*

hESC clumps were transferred to uncoated 35-mm bacterial dishes (SPL Life Science) to be cultured as EBs in suspension culture, then cultured on Matrigel-coated dishes in differentiation medium. The differentiation medium contained the same components as the hESC medium, except that bFGF was omitted and 2% fetal bovine serum was added (Invitrogen).

Transfection of Small Interfering RNAs

The siRNA sequences used in this study are as follows: siRNA-αSIRT1 (forward: 5′-GCA CAG AUC CUC GAA CAA UUC UU-3′, reverse: 5′-GAA UUG UUC GAG GAU CUG UGC UU-3′); siRNA-αSIRT2 (forward: 5′-GAA GAC AUU GCU UAU UGG AUU-3′, reverse: 5′-UCC AAU AAG CAA UGU CUU CUU-3′); and siRNA-Scrambled (forward: 5′-CCU CGU GCC GUU CCA UCA GGU AGU U-3′, reverse: 5′-CUA CCU GAU GGA ACG GCA CGA GGT T-3′). Double-stranded siRNAs were synthesized by Genolution. hESCs were treated with 10 μM ROCK inhibitor Y27632 (EMD Millipore) for 1 hr before harvesting. The cells were dissociated for 4 min using TrypLE Select (Invitrogen) and neutralized by TeSR-E8 cell culture medium. The cells were centrifuged at 100 × *g* for 3 min, washed with 1× PBS, and resuspended in R buffer from the Neon Transfection system (Invitrogen). The reaction contained 100 nM siRNA, and transfections were performed using the Neon Transfection system at 900 V, 20 ms, and 1 pulse. The cells were then immediately plated onto Matrigel-coated plates with Y27632, followed by a medium change the next day.

Apoptosis Analysis

The apoptosis of hESCs was detected using a fluorescein isothiocyanate (FITC) Annexin V Apoptosis Detection Kit (BD Biosciences). Cells were harvested and resuspended in binding buffer at a concentration of 1 × 10^6 cells/mL. A total of 100 μL of the solution was transferred to a 5-mL culture tube and treated with 5 μL each of Annexin V-FITC and PI. The cell suspension was incubated for 15 min at room temperature in the dark and then analyzed by flow cytometry using a FACS LSRII (BD Biosciences).

Western Blotting

Cells treated with various concentrations of Tenovin-6 were lysed with RIPA buffer (Sigma) containing 1× protease inhibitor cocktail (Roche Applied Science). The extracts (20 μg of total protein) were separated on polyacrylamide-SDS gels and transferred to polyvinylidene fluoride membranes (Amersham). The membranes were blocked with a solution containing 2% BSA/1× PBS and incubated overnight with a primary antibody at 4°C. Subsequently, the membranes were incubated with a horseradish peroxidase-conjugated secondary antibody (1:100) (Invitrogen). The reactive proteins were visualized using an ECL substrate solution (Pierce) according

to the manufacturer's instructions. Western blotting was performed using antibodies (Table S6).

Immunocytochemistry

Cells were fixed in 4% paraformaldehyde and permeabilized with 0.1% Triton X-100. The samples then were incubated with blocking buffer (2% BSA in 1× PBS). The cells were incubated overnight with primary antibodies diluted in blocking buffer at 4°C. Primary antibodies (Table S6) to the following proteins were used: SSEA4 (Santa Cruz Biotechnology), cleaved caspase-3 (Cell Signaling Technology), γH2AX (Invitrogen), and SIRT1 (Cell Signaling). The samples were washed with 1× PBS and incubated with fluorescently labeled secondary antibodies for 30 min at room temperature. The secondary antibodies used were Alexa Fluor 488- or Alexa Fluor 594-labeled donkey immunoglobulin G (IgG)/goat IgG (1:1,000; Invitrogen). A cover glass was mounted onto the slides using Vectashield Hardset mounting medium (Vector Laboratories) containing DAPI (Invitrogen). Images were obtained on a DP71 fluorescence microscope (Olympus) and an LSM700 confocal microscope (Carl Zeiss). The Image-iT Dead Green viability stain (Invitrogen) was used to stain dead cells by incubation of the test cells with Dead Green (1:1,000) complete medium.

RNA Preparation and Real-Time qRT-PCR

Total mRNA was extracted using an Easy-Spin Total RNA Purification Kit (iNtRON Biotechnology) and was used for first-strand cDNA synthesis using a PrimeScript RT Reagent Kit (Takara Bio) according to the manufacturer's instructions. Real-time qRT-PCR was performed using SYBR PremixExTaq (Takara Bio). Reactions were performed on a CFX96 Real-Time System (Bio-Rad), and the results were evaluated with CFX real-time detection system software. Quantification was performed by determining the threshold cycle value (C_T), and target genes were normalized to GAPDH (glyceraldehyde-3-phosphate dehydrogenase). Relative target gene expression was quantified using the comparative C_T method. All PCRs were performed in triplicate. Primer sequences are shown in Table S5.

Proteomic Analysis and the Protein-Protein Interaction Network

A proteomic tandem mass spectrometry approach was applied to reveal how proteins were differentially regulated by SIRT1 inhibition in hESCs. To this end, hESCs were treated with Tenovin-6 for 2 hr and the differentially regulated proteins were analyzed with respect to control (DMSO-treated) hESCs. iTRAQ analysis identified a total of 219 differentially regulated proteins (>4-fold), of which 46 (stringent) and 94 (moderate) proteins were downregulated and 23 (stringent) and 56 (moderate) proteins were upregulated. To display the SIRT1-dependent protein regulation in hESCs, we used the STRING database (http:/string-db.org) and KEGG pathway enrichment analyses.

Apurinic/Apyrimidinic Site Analysis

A DNA damage-AP site-Assay kit (Cell-Based) (Abcam) was used for the determination of abasic sites in genomic DNA, according to the manufacturer's instructions. In brief, hESCs were treated with vehicle (control), 100 μM EGCG (positive control), or 5 μM Tenovin-6 for 12 hr. The cells were then stained for AP sites with a DNA damage-AP site-Assay kit. AP sites were labeled with avidin-FITC and directly counted under an Olympus IX 71 microscope.

SUPPLEMENTAL INFORMATION

Supplemental Information includes four figures and six tables and can be found with this article online at http://dx.doi.org/10.1016/j.stemcr.2017.06.001.

AUTHOR CONTRIBUTIONS

D.-Y.H. and D.-W.K. designed the study; J.J., Y.J.H., H.-J.C., J.P., and B.L. performed the experiments; and D.-Y.H., J.J., and D.-W.K. wrote the manuscript.

ACKNOWLEDGMENTS

D.-W.K. and J.J. were supported by grants from the National Research Foundation of Korea (Bio and Medical Technology Development Program: 2012M3A9B4028631, 2012M3A9C7050126, and 2012M3A9C6049724) and the Korean Ministry of Health and Welfare (HI15C0916). D.-Y.H. was supported by a grant (2012M3A9C7050130) from the MSIP. We thank Dong-Su Jang, MFA (Medical Illustrator, Medical Research Support Section, Yonsei University College of Medicine) for his help with the illustrations.

Received: September 4, 2016
Revised: June 1, 2017
Accepted: June 1, 2017
Published: July 6, 2017

REFERENCES

Becker, K.A., Ghule, P.N., Therrien, J.A., Lian, J.B., Stein, J.L., van Wijnen, A.J., and Stein, G.S. (2006). Self-renewal of human embryonic stem cells is supported by a shortened G1 cell cycle phase. J. Cell Physiol. *209*, 883–893.

Calvanese, V., Lara, E., Suarez-Alvarez, B., Abu Dawud, R., Vazquez-Chantada, M., Martinez-Chantar, M.L., Embade, N., Lopez-Nieva, P., Horrillo, A., Hmadcha, A., et al. (2010). Sirtuin 1 regulation of developmental genes during differentiation of stem cells. Proc. Natl. Acad. Sci. USA *107*, 13736–13741.

Chung, S., Shin, B.S., Hedlund, E., Pruszak, J., Ferree, A., Kang, U.J., Isacson, O., and Kim, K.S. (2006). Genetic selection of sox1GFP-expressing neural precursors removes residual tumorigenic pluripotent stem cells and attenuates tumor formation after transplantation. J. Neurochem. *97*, 1467–1480.

De Bonis, M.L., Ortega, S., and Blasco, M.A. (2014). SIRT1 is necessary for proficient telomere elongation and genomic stability of induced pluripotent stem cells. Stem Cell Rep. *2*, 690–706.

Demple, B., and Harrison, L. (1994). Repair of oxidative damage to DNA: enzymology and biology. Annu. Rev. Biochem. *63*, 915–948.

Elangovan, S., Ramachandran, S., Venkatesan, N., Ananth, S., Gnana-Prakasam, J.P., Martin, P.M., Browning, D.D., Schoenlein, P.V., Prasad, P.D., Ganapathy, V., et al. (2011). SIRT1 is essential for oncogenic signaling by estrogen/estrogen receptor alpha in breast cancer. Cancer Res. *71*, 6654–6664.

Filion, T.M., Qiao, M., Ghule, P.N., Mandeville, M., van Wijnen, A.J., Stein, J.L., Lian, J.B., Altieri, D.C., and Stein, G.S. (2009). Survival responses of human embryonic stem cells to DNA damage. J. Cell Physiol. *220*, 586–592.

Hable, V., Drexler, G.A., Bruning, T., Burgdorf, C., Greubel, C., Derer, A., Seel, J., Strickfaden, H., Cremer, T., Friedl, A.A., et al. (2012). Recruitment kinetics of DNA repair proteins Mdc1 and Rad52 but not 53BP1 depend on damage complexity. PLoS One *7*, e41943.

Houtgraaf, J.H., Versmissen, J., and van der Giessen, W.J. (2006). A concise review of DNA damage checkpoints and repair in mammalian cells. Cardiovasc. Revasc Med. *7*, 165–172.

Huffman, D.M., Grizzle, W.E., Bamman, M.M., Kim, J.S., Eltoum, I.A., Elgavish, A., and Nagy, T.R. (2007). SIRT1 is significantly elevated in mouse and human prostate cancer. Cancer Res. *67*, 6612–6618.

Hwang, D.Y., Kim, D.S., and Kim, D.W. (2010). Human ES and iPS cells as cell sources for the treatment of Parkinson's disease: current state and problems. J. Cell Biochem. *109*, 292–301.

Kaina, B. (2003). DNA damage-triggered apoptosis: critical role of DNA repair, double-strand breaks, cell proliferation and signaling. Biochem. Pharmacol. *66*, 1547–1554.

Kalle, A.M., Mallika, A., Badiger, J., Alinakhi, Talukdar, P., and Sachchidanand. (2010). Inhibition of SIRT1 by a small molecule induces apoptosis in breast cancer cells. Biochem. Biophys. Res. Commun. *401*, 13–19.

Khanna, K.K., and Jackson, S.P. (2001). DNA double-strand breaks: signaling, repair and the cancer connection. Nat. Genet. *27*, 247–254.

Kinner, A., Wu, W., Staudt, C., and Iliakis, G. (2008). Gamma-H2AX in recognition and signaling of DNA double-strand breaks in the context of chromatin. Nucleic Acids Res. *36*, 5678–5694.

Kojima, K., Ohhashi, R., Fujita, Y., Hamada, N., Akao, Y., Nozawa, Y., Deguchi, T., and Ito, M. (2008). A role for SIRT1 in cell growth and chemoresistance in prostate cancer PC3 and DU145 cells. Biochem. Biophys. Res. Commun. *373*, 423–428.

Kuzmichev, A., Margueron, R., Vaquero, A., Preissner, T.S., Scher, M., Kirmizis, A., Ouyang, X., Brockdorff, N., Abate-Shen, C., Farnham, P., et al. (2005). Composition and histone substrates of polycomb repressive group complexes change during cellular differentiation. Proc. Natl. Acad. Sci. USA *102*, 1859–1864.

Lain, S., Hollick, J.J., Campbell, J., Staples, O.D., Higgins, M., Aoubala, M., McCarthy, A., Appleyard, V., Murray, K.E., Baker, L., et al. (2008). Discovery, in vivo activity, and mechanism of action of a small-molecule p53 activator. Cancer Cell *13*, 454–463.

Lee, Y.L., Peng, Q., Fong, S.W., Chen, A.C., Lee, K.F., Ng, E.H., Nagy, A., and Yeung, W.S. (2012). Sirtuin 1 facilitates generation of induced pluripotent stem cells from mouse embryonic fibroblasts through the miR-34a and p53 pathways. PLoS One *7*, e45633.

Lin, Z., and Fang, D. (2013). The roles of SIRT1 in cancer. Genes Cancer *4*, 97–104.

Liu, J.C., Lerou, P.H., and Lahav, G. (2014). Stem cells: balancing resistance and sensitivity to DNA damage. Trends Cell Biol. *24*, 268–274.

Momcilovic, O., Knobloch, L., Fornsaglio, J., Varum, S., Easley, C., and Schatten, G. (2010). DNA damage responses in human induced pluripotent stem cells and embryonic stem cells. PLoS One *5*, e13410.

Oberdoerffer, P., Michan, S., McVay, M., Mostoslavsky, R., Vann, J., Park, S.K., Hartlerode, A., Stegmuller, J., Hafner, A., Loerch, P., et al. (2008). SIRT1 redistribution on chromatin promotes genomic stability but alters gene expression during aging. Cell *135*, 907–918.

Ou, X., Chae, H.D., Wang, R.H., Shelley, W.C., Cooper, S., Taylor, T., Kim, Y.J., Deng, C.X., Yoder, M.C., and Broxmeyer, H.E. (2011). SIRT1 deficiency compromises mouse embryonic stem cell hematopoietic differentiation, and embryonic and adult hematopoiesis in the mouse. Blood *117*, 440–450.

Ou, X., Lee, M.R., Huang, X., Messina-Graham, S., and Broxmeyer, H.E. (2014). SIRT1 positively regulates autophagy and mitochondria function in embryonic stem cells under oxidative stress. Stem Cells *32*, 1183–1194.

Rich, T., Allen, R.L., and Wyllie, A.H. (2000). Defying death after DNA damage. Nature *407*, 777–783.

Richardson, C., and Jasin, M. (2000). Frequent chromosomal translocations induced by DNA double-strand breaks. Nature *405*, 697–700.

Roos, W.P., and Kaina, B. (2006). DNA damage-induced cell death by apoptosis. Trends Mol. Med. *12*, 440–450.

Sakaguchi, K., Herrera, J.E., Saito, S., Miki, T., Bustin, M., Vassilev, A., Anderson, C.W., and Appella, E. (1998). DNA damage activates p53 through a phosphorylation-acetylation cascade. Genes Dev. *12*, 2831–2841.

Saretzki, G., Armstrong, L., Leake, A., Lako, M., and von Zglinicki, T. (2004). Stress defense in murine embryonic stem cells is superior to that of various differentiated murine cells. Stem Cells *22*, 962–971.

Simic, P., Zainabadi, K., Bell, E., Sykes, D.B., Saez, B., Lotinun, S., Baron, R., Scadden, D., Schipani, E., and Guarente, L. (2013). SIRT1 regulates differentiation of mesenchymal stem cells by deacetylating beta-catenin. EMBO Mol. Med. *5*, 430–440.

Sokolov, M.V., Panyutin, I.V., and Neumann, R.D. (2012). Unraveling the global microRNAome responses to ionizing radiation in human embryonic stem cells. PLoS One *7*, e31028.

Sykes, S.M., Mellert, H.S., Holbert, M.A., Li, K., Marmorstein, R., Lane, W.S., and McMahon, S.B. (2006). Acetylation of the p53 DNA-binding domain regulates apoptosis induction. Mol. Cell *24*, 841–851.

Tang, Y., Luo, J., Zhang, W., and Gu, W. (2006). Tip60-dependent acetylation of p53 modulates the decision between cell-cycle arrest and apoptosis. Mol. Cell *24*, 827–839.

Tang, S., Huang, G., Fan, W., Chen, Y., Ward, J.M., Xu, X., Xu, Q., Kang, A., McBurney, M.W., Fargo, D.C., et al. (2014). SIRT1-mediated deacetylation of CRABPII regulates cellular retinoic acid signaling and modulates embryonic stem cell differentiation. Mol. Cell *55*, 843–855.

Terada, N., Hamazaki, T., Oka, M., Hoki, M., Mastalerz, D.M., Nakano, Y., Meyer, E.M., Morel, L., Petersen, B.E., and Scott, E.W.

(2002). Bone marrow cells adopt the phenotype of other cells by spontaneous cell fusion. Nature *416*, 542–545.

Wang, R.H., Sengupta, K., Li, C., Kim, H.S., Cao, L., Xiao, C., Kim, S., Xu, X., Zheng, Y., Chilton, B., et al. (2008). Impaired DNA damage response, genome instability, and tumorigenesis in SIRT1 mutant mice. Cancer Cell *14*, 312–323.

Westmoreland, J.W., and Resnick, M.A. (2013). Coincident resection at both ends of random, gamma-induced double-strand breaks requires MRX (MRN), Sae2 (Ctp1), and Mre11-nuclease. PLoS Genet. *9*, e1003420.

Wilson, K.D., Sun, N., Huang, M., Zhang, W.Y., Lee, A.S., Li, Z., Wang, S.X., and Wu, J.C. (2010). Effects of ionizing radiation on self-renewal and pluripotency of human embryonic stem cells. Cancer Res. *70*, 5539–5548.

Ying, Q.L., Nichols, J., Evans, E.P., and Smith, A.G. (2002). Changing potency by spontaneous fusion. Nature *416*, 545–548.

Yoo, J., Kim, H.S., and Hwang, D.Y. (2013). Stem cells as promising therapeutic options for neurological disorders. J. Cell Biochem. *114*, 743–753.

Zhang, Z.N., Chung, S.K., Xu, Z., and Xu, Y. (2014). Oct4 maintains the pluripotency of human embryonic stem cells by inactivating p53 through Sirt1-mediated deacetylation. Stem Cells *32*, 157–165.